Proc. CIBSE A: Building Serv. Eng. Res. Technol. **19**(4) 213–218 (1998) Printed in Great Britain B464

Summary Particle loss augmentation in turbulent flow was studied experimentally. Experiments were performed in a 150 mm square ventilation duct. Small tracer particles of size ranging from 0.7–7.1 μm were used to study deposition enhancement with streamwise-periodic disturbances mounted on one of the principal walls, under turbulent flow. A new and highly sensitive analytical technique was adopted to determine the spatial mass flux along the ribbed duct. On some surfaces, particle deposition enhancement as much as seven times higher than on smooth surfaces was observed. Periodic averages of mass transfer coefficients for different particle sizes were evaluated. The friction factor was approximately three times the smooth duct value. Efficiency indexes, based on equal fan power, were determined for all particle sizes.

Turbulent particle loss augmentation in a ventilation duct

A C K Lai† BEng MPhil PhD DIC
Built Environment Group, Imperial College Centre for Environmental Technology, Imperial College, London SW7 2BP, UK

Received 4 September 1997, in final form 19 February 1998

List of symbols

A Area (m^2)
C_∞ Particle free stream concentration (particle m^{-3})
D_e Hydraulic mean diameter (m)
$F(n)$ Energy contribution from frequency n
f Friction factor
H Height of rib (m)
$\mathcal{J}$ Particle transport per unit area per unit time, mass deposition flux (particle $m^{-2}s^{-1}$)
k Mass transfer coefficient (m s^{-1})
L Eddy length scale (m)
ΔL Distance between two pitot tubes (m)
M Mass of particle (g)
P Pitch length of ribbed surface (m)
ΔP Differential pressure loss (Pa)
Q Air flow through air samplers (m^3)
t Time (s)
U Mean fluid velocity (m s^{-1})
ρ Density of fluid (kg m^{-3})
ζ Efficiency index
Re Reynolds number

Subscripts

r rough
s smooth

1 Introduction

In the urban environment, indoor air pollution has become an issue of major concern over the past few decades. Humans spend 70–90%[1] of their time indoors and are subjected to infiltrated outdoor air which is heavily polluted by vehicle exhausts and by industrial emissions[2]. For mechanically ventilated buildings, the most common method for removing particulate pollutants is by filtration at the air intake points. This obviously incurs significant energy costs.

The enhancement of small-particle deposition along the length of a ventilation duct may present an effective alternative to filtration, or may complement the current filtration method, e.g. electrostatic air precipitation. Particle deposition may be enhanced through roughening the duct surface. This a strategy is widely adopted in heat flux transfer enhancement (e.g. in gas turbine blade and nuclear reactor cooling designs). Hence, the first logical step in studying the possible mechanisms of small-particle deposition enhancement is to make use of the well-established mechanisms of heat transfer enhancement. One of the most popular and best established methods for enhancing the heat transfer from a surface is to roughen it by a pattern of repeated ribs.

Theoretical and experimental studies of small particle deposition on ribbed surfaces are rare. Li *et al.*[3] used computer simulation to predict the dispersion and deposition of particles in a duct with large rectangular and trapezoidal obstructing blocks. Their results show that large numbers of particles deposit on the blocks due to impaction and interception. Wells and Chamberlain[4] measured the deposition velocity of small particles on a small vertical tube with smooth and rough surfaces (the rough surface being filter paper). Particle deposition was enhanced by two orders of magnitude. Hahn *et al.*[5] carried out experiments to measure the deposition of sub-micrometre particles of size ranging from 0.04 to 0.2 μm on a small ribbed pipe, for three values of rib separation. The results correlated well with the heat transfer analogue.

Studies have shown that heat (mass) transfer‡ is strongly influenced by mean and turbulent flow parameters, and this finding has relevance to the analogy: particle deposition. However, there are obviously differences between heat (mass) transfer and particle deposition processes: impaction and interception may play substantial roles for super-micrometre aerosol particle deposition, and these effects cannot be investigated by using heat (mass) transfer techniques.

The above discussion indicates that, to date, there are no available experimental data for small-particle deposition enhancement (at sizes ranging from sub- to super-micrometre) on ribbed surfaces in a turbulent flow regime. The objective of the current work is to study particle deposition enhancement along a rib-roughened duct under turbulent flow conditions, observing the spatial distributions of particle deposition in order to gain more insight into the actual enhancement processes. This is a key step in modifying current filtration devices, such as the electrostatic air precipitator, for mechanical ventilation ducts. Another objective is to

†Present address: Department of Civil and Environmental Engineering, 631 Davis Hall, University of California, Berkeley, CA 94720-1710, USA

‡Mass transfer in this context refers to transfer of inertialess mass molecules (or ions) and is different from particle transfer.

evaluate the suitability (in terms of energy efficiency) of such a surface for air cleaning.

2 Experimental apparatus, procedure and data reduction

2.1 Experimental set-up

The experimental ribbed duct system is shown schematically in Figure 1. The square duct system comprises ten galvanised and two Perspex channels. The internal cross sectional dimensions of the channels are 150 × 150 mm and the length of each section is approximately 500 mm. A typical arrangement is Perspex square ribs of height H = 6 mm, placed transversely into a duct of hydraulic diameter D_e, between prescribed intervals of pitch length P = 60 mm.

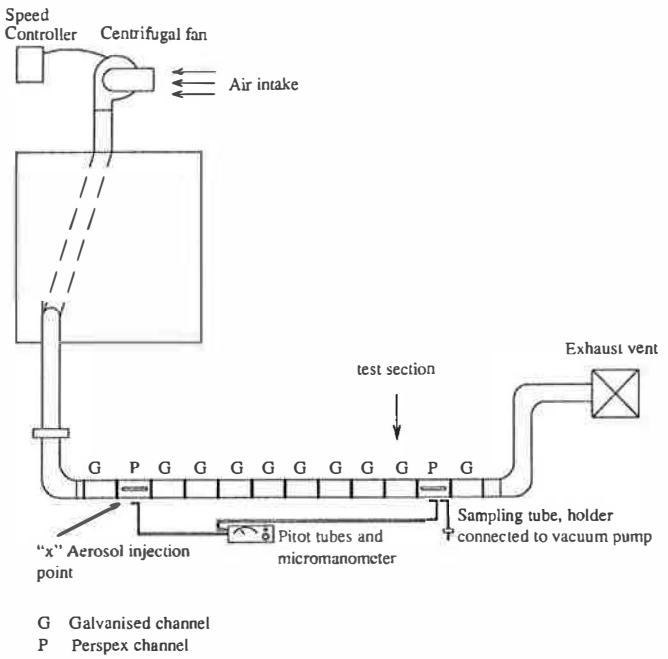

Figure 1 Schematic diagram of experimental system for rectangular ventilation duct

Traditionally, two parameters are used to characterise the ribbed duct, i.e. P/H and H/D_e. Both parameters strongly affect the heat/mass enhancement performance. Heat transfer increases with increasing pressure drop of the fluid flow. Research has shown that a P/H value around 10 optimises performance, i.e. a high heat flux enhancement ratio with a low pressure increment ratio[6,7], so P/H was fixed at 10 in the present work.

The test section was located at the tenth galvanised channel (Figure 1). It was not necessary to cover the whole duct system with the ribbed elements to create a fully developed periodic flow pattern. Liou *et al.*[8] have shown that the flow reaches a fully developed state after the tenth ribs. In the present work fourteen ribs were placed upstream of the measurement section. Thin acetate sheets were fitted to cover three pitch lengths (21 samples for each run). In order to determine the deposition enhancement efficiency, particle deposition on a smooth surface was also tested. Fifteen 13 × 25 mm thin acetate sheets were cut and glued along the central line of a plain Perspex plate.

Spatial distributions of the particle flux can be determined by the following sampling arrangement. Separate thin acetate sheets with a thickness less than 0.1 mm were cut to fit the frontal, top and backward regions of a rib and fixed by removable tape. Four more acetate sheets were cut and fitted onto the smooth separation region between two successive ribs (unribbed region). With the aid of this arrangement, seven samples could be obtained for each pitch length for analysis. Figure 2 depicts the arrangement of samples along a pitch of ribbed duct.

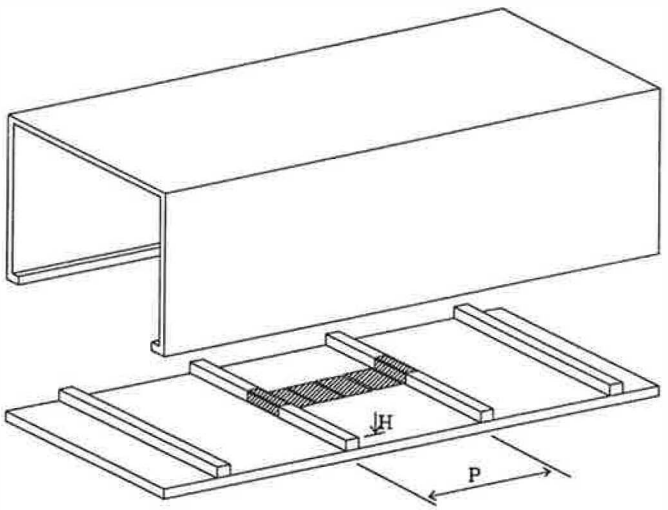

Figure 2 Arrangement of two-dimensional rib elements along ventilation duct. The shaded parts are thin acetate sheets glued onto the surfaces for spatial analysis purposes.

2.2 Analytical method

Earlier researchers have used the fluorescence spectroscopy method[9–10]. However, this is a bulk analytical technique and is not suitable for providing information on the spatial distribution of deposited particles. Neutron activation analysis, with tracer-labelled small particles, was employed to study deposition on ribbed surfaces in turbulent flow conditions. Details of the technique can be found elsewhere[11] and its application here is described only briefly.

Neutron activation analysis (NAA) is the detection technique used in this work. The Rare earth elements dysprosium ^{164}Dy and indium ^{115}In were used as tracers. Both exist naturally in a stable state but become unstable (i.e. radioactive) when bombarded with neutrons. They decay to other stable nuclei with characteristic half-lives (1.26 minutes for dysprosium and 54 minutes for indium) emitting radiation of characteristic energy (gamma rays of 108 keV for Dy and of 416 keV for In). After a period of particle deposition in a test duct, irradiation of tracer particle-bearing materials (such as air filter papers or samples of thin acetate sheet), followed by gamma spectrometry, allows a quantitative determination of the particle mass present. Since dysprosium and indium occur naturally in low concentrations, the possibility of analytical interference from particle-bearing media is minimised. Also, both elements are highly susceptible to neutrons excitation. A dysprosium mass of the order of 1×10^{-10} g can easily be measured after one minute's irradiation in a neutron flux of 2×10^{12} neutrons $cm^{-2}s^{-1}$, hence the method is very sensitive to the number of particles deposited.

Four tracer-labelled particle sizes were prepared for this work: 0.7, 2.5 4.5 and 7.1 μm. The sizes span the diffusion-dominated regime and the sedimentation-dominated regime. The super-micrometre particles used were porous silica

spheres. The particles were dispersed using a powder dispersion generator and were labelled with dysprosium. The submicrometre particles were generated directly by nebulising a solution of indium.

2.3 Experimental procedure

Anti-static spray was applied to the samples immediately before each experiment. In addition, in order to eliminate particulate resuspension, a thin coating of liquid paraffin oil was applied evenly to the sample surfaces. Air at room temperature was drawn into the ductwork and the flow speed was fixed, by a variable-speed controller, at an average of 4.4 m s^{-1} (Reynolds number = 44 000). Small particles were injected into the upstream Perspex duct (marked as × in Figure 1). Owing to the high detection sensitivity of NAA, each experiment ran for only 15 to 20 minutes.

The Reynolds number and pressure drop for both smooth and rough surfaces were calculated using pitot-static tube(s) connected to a micromanometer. The pressure drop across the smooth surface was measured by the static pressure difference across two Perspex channels, since in measuring the total pressure difference an error would have resulted due to the disturbance caused by velocity fluctuation. Similar measuring procedures were employed for the rough surfaces, with the ribbed elements in place. The Reynolds number was measured by locating a pitot-static tube in the central line of a downstream Perspex channel.

2.4 Data reduction

The friction factor for both smooth and ribbed surfaces were calculated by measuring the pressure difference across two Perspex channels and can be written as

$$f = (D_e/4)\Delta P/{}^1/_2 \rho U^2 \Delta L \quad (1)$$

where ρ is the air density, U is the bulk mean velocity and $\Delta P/\Delta L$ is the pressure loss across the length by which the two pitot tubes are separated. The measured result for the smooth surface was compared with the Blasius empirical expression which is given by

$$f = 0.0791/\mathrm{Re}^{0.25} \quad (2)$$

The mass transfer coefficient k (m s^{-1}) is the key parameter to be determined and is defined as

$$k = \mathcal{J}/C_\infty \quad (3)$$

where $\mathcal{J}$ is the particle flux to the surface per unit time and C_∞ is the particle free stream concentration.

As outlined in the previous section, neutron activation analysis was used to determine the tracer particle mass on the air and surface samples. $\mathcal{J}$ and C_∞ were evaluated as

$$\mathcal{J} = M_{\mathrm{acetate}}/A_{\mathrm{acetate}} \quad (4)$$

$$C_\infty = M_{\mathrm{filter}}/Q \quad (5)$$

where M_{acetate}, M_{filter} are the particle masses detected on the acetate and filter paper samples respectively. t is the sampling time, A_{acetate} is the area of the acetate sample and Q is the volumetric flow rate of the air samples.

Ignoring other minor error sources (errors in measurement of t and Q were less than 0.5%), the principal errors arise from M_{acetate} and M_{filter}. The representative uncertainty for both is 5%, and the overall uncertainty estimated for the mass transfer coefficient was less than 7% via the estimation method of Kline and McClintock[12].

3 Results and discussion

3.1 Reynolds number

Since only the flow velocity at the centre of the downstream Perspex channel was measured, the average Reynolds number was estimated. Ali[13] measured the ratio of average to centre velocity as 0.77 in his 150 mm square channel for Reynolds number 3.42×10^5. Based on that ratio, the average Re for the present work was 4.4×10^4. Although the Reynolds number is about one order of magnitude higher than that used in this work, it is believed that the ratio should be similar because the two experiments were carried out in fully turbulent regimes.

3.2 Friction factor

The friction factor for the smooth surface, f_{smooth}, was measured as 5×10^{-3}. The Blasius calculation was 5.48×10^{-3}. Many pressure-drop measurements have been made in channels with two ribbed surfaces[14–15] due to the wide practical application of such channels. However, few measurements of friction factor for a single ribbed surface, frough, with H/D_e, P/H values and a Reynolds number range similar to that for the present work are available. Chandra and Cook[16] measured the ratio $f_{\mathrm{rough}}/f_{\mathrm{smooth}}$ for a single ribbed surface with parameters similar to those for this work; the ratio is 3.2 in the present work and a value of approximately 3.4 was deduced from a value in their paper. The friction factor calculated from the model[17] for the present rib parameters and flow speed gives an increment ratio of 3.0.

3.3 Mass transfer coefficient on smooth surfaces

Particle deposition velocities on smooth surfaces have been reported widely in the literature. However, measurements in a large channel are rare. Table 1 shows experimental aerosol deposition velocity data for the bottom floor on a smooth surface, and shows a comparison with the data of Sehmel[18] whose measurements were in a wind tunnel (0.6 × 0.6 m^2).

Table 1 indicates that, apart from the data for 0.7 μm particles, all the other data agree well with Sehmel's measurements. This discrepancy may be attributable to different channel sizes and the flow speeds in the present work. The average flow speed chosen for comparison is 2.2 m s^{-1} and the corresponding Re is 9.2×10^4. The Prandtl eddy length scales L for the present work and for the Sehmel's work are 12 mm and 48 mm respectively. A smaller eddy length scale aids the transportation of aerosol particles closer to the surface and hence results in greater deposition.

Table 1 Measured mass transfer coefficient on the horizontal surface of smooth duct

Particle size (μm)	Mass transfer coefficient (m s^{-1})	
	Measured	From Reference 18
0.7	5.9×10^{-4}	2.5×10^{-5}
2.5	8.8×10^{-4}	3.0×10^{-4}
4.5	5.0×10^{-3}	1.5×10^{-3}
7.1	8.8×10^{-3}	3.0×10^{-3}

The turbulent frequency spectrum provides a more detailed view of the flow structure than a single number such as the scale L. Dryden[19] gave an equation for the eddy spectrum

$$UF(n)/L = 4/[(1 + 4\pi^2 n^2 (L/U^2)] \quad (6)$$

where n is the frequency of the eddy and $F(n)$ is the energy contribution from the frequency n.

As the magnitude of L/U decreases, the probability of high frequency oscillations increases rapidly. Therefore the percentage of small eddies also increases. In the configuration of Sehmel[18], L/U is about 0.022 whereas in the present work, the L/U ratio is only 0.0027. This higher frequency oscillation affects sub-micrometre particle deposition more readily than super-micrometre particle deposition. This probably explains the large difference for the 0.7 μm particle measured in the present work and in Sehmel's work.

3.4 *Mass transfer coefficient on a ribbed surface*

Figure 3 shows the measured particle deposition enhancement ratio, compared with the values for the smooth surface. For 0.7 μm particles, an enhancement ratio of approximately 6.5 is observed at the frontal surfaces; this reduces to two along the smooth surfaces between ribs.

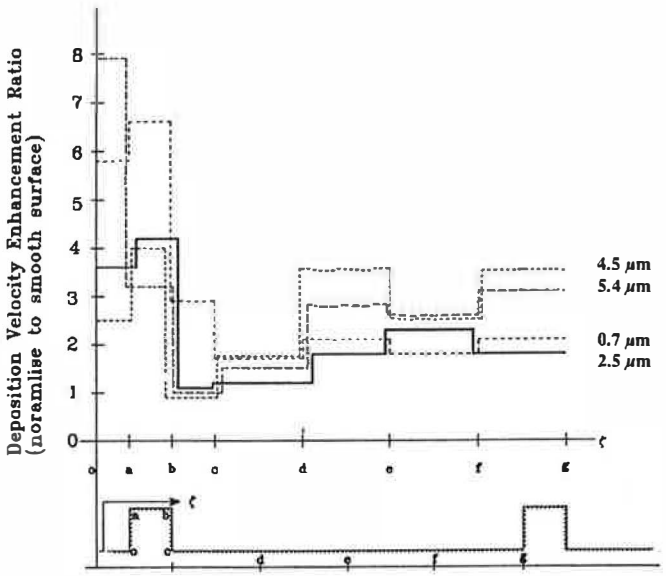

Figure 3 Measured spatial distribution of relative aerosol deposition velocity along one pitch of ribbed surfaces

For 2.5 μm particles, it can be seen that the enhancement ratio reduces to four at the top surface. Another peak occurs at surface e–f, due to the high turbulent intensity associated with flow reattachment in this region. For the 4.5 μm particles, the enhancement ratio reduces further to less than three at the frontal surfaces.

It can be seen from Figure 3 that for 7.1 μm particles direct impaction (due to inertia) of particles at the frontal surface makes the enhancement ratio close to eight. The deposition of particle on the front surface of bluff body (like a rib) is quite well understood[20]. When approaching the front surface, due to its own inertia, the particle cannot follow the trajectory of the fluid exactly, but tends to travel in a straight line and strike onto the front surfaces. Experimental work[20] and computation[3] both demonstrated that particle deposition rate increasing rapidly after a certain range of particle sizes.

It is interesting to compare the present results with those of heat and mass transfer studies on similar ribbed surfaces. Hahn *et al.*[5] demonstrated that for the very small particles they tested, the mass transfer coefficient showed good correlation with the heat transfer analogue. In the present work, the particle sizes tested were 7 to 170 times hat used by Hahn *et al.* In the literature, various techniques have been used employed to measure heat transfer coefficients. Liou and Hwang[15] measured the heat transfer coefficient by holographic interferometry. Kukreja *et al.*[21] measured the mass transfer coefficient by naphthalene sublimation, whereas Berger and Hau[22] measured the coefficient by an electrochemical method. The results of these studies are compared with those of the present work (0.7 and 7.1 μm particles) in Table 2.

The comparison shows that on ribbed surfaces, the small particle transfer process is very different to that of heat transfer. Significantly higher enhancement ratios are found at the frontal and top surfaces. The likely reason for this is particle inertia. Along the smooth surfaces between ribs, the enhancement ratios for 0.7 μm particles agree quite well with the heat (mass) transfer measurements, i.e. in all cases the peak value is at position d–e which corresponds to the location of the highest turbulent intensity. For 7.1 μm particles, the highest peak along smooth surfaces between the ribs is at f–g instead of d–e; this may be due to a vortex formed by the presence of the downstream rib, which enhances particle deposition.

In order to draw an effective analogy between heat and mass transfers, the diffusivities of each should be of comparable magnitude. In the case of particles in a gas stream, however, the ratio of the Schmidt number to the Prandtl number can be of the order of 10^5. Under such circumstances, the analogy should be applied with caution. In addition, each small particle, unlike naphthalene vapour, weighs more than ten thousand times as much as an air molecule. It is to be anticipated that the transfer mechanism will not be exactly the same, especially for large particles, for which inertial effect (impaction) plays an important role.

3.5 *Efficiency ratio*

The effectiveness with which a ribbed surface enhances particle deposition is coupled with a pressure drop across that surface. There are several methods to evaluate the performance of the ribbed surfaces by taking into account both mass flux gain due to the enhanced particle transfer and the energy loss due to the increase in friction factor. In this work the primary objective is to evaluate the practical feasibility of the ribbed duct. Therefore the efficiency index is chosen by comparing the particle transfer coefficient between rough and smooth

Table 2 Comparison of present results with those from heat/mass transfer studies

Parameter	Reference	P/H	H/D_e	Re	Size (μm)	Front (o–a)	Top (a–b)	Back (b–c)	c–d	d–e	e–f	f–g
Heat	15†	10	0.081	10200	—	2.5	2.5	1.0	1.3	2.2	2.0	2.0
Mass	21†	10	0.0625	45000	—	—	—	—	1.5	2.4	2.2	2.4
Mass	22†	10	0.0364	32090	—	—	3.2	—	2.0	3.1	2.6	2.5
Particle	Present	—	—	—	0.7	5.8	6.6	2.9	1.7	2.1	1.8	2.1
Particle	Present	—	—	—	7.1	8.0	3.2	1.0	1.5	2.8	2.6	3.1

†Estimated from literature values. Maximum errors are believed to be within ±0.3.

ducts under the same fan power. According to this criterion, an efficiency index (at equal fan power) is defined as follows[23]:

$$\zeta = (k_{rough}/k_{smooth})/(f_{rough}/f_{smooth})^{1/3} \quad (6)$$

where k_{rough} and k_{smooth} are the average mass transfer coefficient along one pitch of the ribbed surface and the smooth surface respectively, f_{rough}/f_{smooth} is the friction factor ratio of rough to smooth surfaces and was measured as 3.2 in the present work.

Figure 4 depicts the efficiency index calculated by equation 6. The maximum efficiencies correspond to particle sizes of 0.7 and 7.1 μm, for which turbulence or sedimentation are the dominant deposition enhancement processes. Since the efficiencies are all greater than unity, this suggests that the ribbed surface is an energy efficient method of enhancing particle deposition.

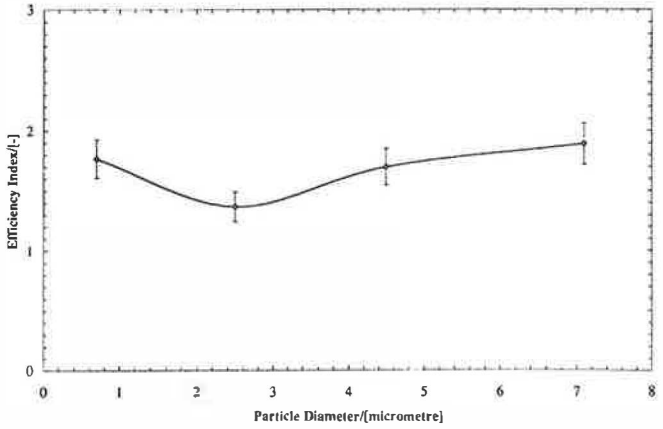

Figure 4 Efficiency indexes of four particle sizes for ribbed surfaces

4 Conclusion

The motivation of this study was to investigate particle deposition along a roughened surface, and how to modify or improve the capture efficiency of current designs of some common devices such as the electrostatic precipitator. It is not intended to existing filters.

Particle deposition enhancement on ribbed surfaces was studied for a periodic fully developed turbulent flow field in a channel with one surface (horizontal and upward facing) roughened by ribs, using neutron-activatable tracer-labelled particles. The key conclusions are as follows.

(*a*) Turbulence enhances sub-micrometre particle deposition at the back surface of a rib. This effect was not observed for super-micrometre particles.

(*b*) Particle deposition enhancement ratios for four particle sizes were determined. For sub-micrometre particles, it is found that turbulent intensity enhances deposition effectively, especially for the frontal and top surfaces of the rib. The ratios relative to the smooth surface values are six and seven respectively. For the super-micrometre particles, impaction is found to be an effective mechanism to enhance deposition.

(*c*) Relative to a smooth duct, the presence of repeated ribs on a single surface causes a pressure increment of 3.2. The average efficiency indices over one pitch for four particle sizes vary from 1.4 to 1.9. The highest efficiency indices observed are for the smallest and largest particle sizes studied.

(*d*) The measured results do not correlte well with heat transfer measurements. High mass transfer coefficients were found at the frontal surfaces of ribs. A plausible explanation is particle inertia.

Further work will include experiments on those smaller particle sizes which are believed to affect human health adversely, and are difficult to remove by conventional devices. Particle retention power on the ribbed surfaces will also be addressed.

Acknowledgement

The author expresses his great appreciation to The Croucher Foundation, Hong Kong for supporting his research at Imperial College.

References

1 Raunemaa T, Kulmala M, Saari H, Olin M and Kulmala M H Indoor air aerosol model: transport and deposition of fine and coarse particles *Aerosol Sci. Technol.* **11**(1) 11–25 (1989)

2 Li C S Elemental composition of residential indoor PM10 in the urban atmospheric of Taipei *Atmos. Envir.* **28**(19) 3139–3144 (1994)

3 Li A, Ahmadi G, Bayer R G and Gaynes M A Aerosol particle deposition in an obstructed turbulent duct flow *J. Aerosol Sci.* **25**(1) 91–112 (1994)

4 Wells A C and Chamberlain A C Transport of small particles to vertical surfaces *Brit. J. Phys.* **18**(12) 1793–1799 (1967)

5 Hahn L A, Stukel J J, Leong K H and Hopke P K Turbulent deposition of submicron particles on rough walls *J. Aerosol Sci.* **16**(1) 81–86 (1985)

6 Okamoto S, Seo S, Nakaso K and Kawai I Turbulent shear flow and heat transfer over the repeated two-dimensional square ribs on ground plane *ASME Trans. J. Fluid Eng.* **115**(4) 631–637 (1993)

7 Liou T M, Hwang J J and Chen S H Simulation and measurement of enhanced turbulent heat transfer in a channel with periodic ribs on one principal wall *Int. J. Heat Mass Transfer* **36**(2) 507–517 (1993)

8 Liou T M, Wang W B and Chang Y J Holographic interferometry study of spatially periodic heat transfer in a channel with ribs detached from one wall *ASME Trans. J. Heat Transfer* **117**(1) 32–39 (1995)

9 Liu B Y H and Agarwal J K Experimental observation of aerosol deposition in turbulent flow *J. Aerosol Sci.* 5(2) 145–155 (1974)

10 Muyshondt A, Nakaso K and Kawai I Turbulent deposition of aerosol particles in large transport tubes *Aerosol Sci. Technol.* **24**(2) 107–116 (1993)

11 Lai C K PhD thesis, Imperial College of Science, Technology and Medicine, University of London (1997)

12 Kline S J and McClintock F A Describing uncertainties in single-sample experiments *Mech. Eng.* **75**(1) 3–8 (1953)

13 Ali M A T PhD thesis, Imperial College of Science, Technology and Medicine, University of London (1980)

14 Han J C Heat transfer and friction in channels with two opposite rib-roughened walls *ASME Trans. J. Heat Transfer* **106**(4) 774–781 (1984)

15 Liou T M and Hwang J J Turbulent heat transfer augmentation and friction in periodic fully developed channel flows *ASME Trans. J. Heat Transfer* **114**(1) 56–64 (1992)

16 Chandra P R and Cook M M Effect of the number of channel ribbed walls on heat transfer and friction characteristics of turbulent flows *Proc. 6th Joint Conf. AIAA/ASME Thermophysics and Heat Transfer, Colorado Springs, USA* **HTD** 271 pp201–209 (1994)

17 Tran L T Turbulent friction and heat transfer calculations of a rectangular duct with repeated ribs on two opposite walls *Proc. ASME Winter Annual Meeting, New Orleans, USA* (1993)

18 Sehmel G A Particle diffusivities and deposition velocities over a horizontal smooth surface *J. Colloid Interface Sci.* **37**(4) 891–906 (1971)

19 Dryden H L *A review of the statistical theory of turbulence in Turbulence* in *Classic Papers on Statistical Theory* (New York: Interscience) p115 (1961)

20 Vincent J H and Humphries W The collection of airborne dusts by bluff bodies *Chem. Eng. Sci.* **33**(8) 1147–1155 (1978)

21 Kukreja R T, Lau S C and McMillin R D Local heat/mass transfer distribution in a square channel with full and v-shaped ribs *Int. J. Heat Mass Transfer* **36**(8) 2013–2020 (1993)

22 Berger F P and Hau K-F F-L Local mass/heat transfer distribution on surfaces roughened with small square rib *Int. J. Heat Mass Transfer* **22** 1645–1656 (1979)

23 Vilemas J V and Simonis V M Heat transfer and friction of rough ducts carrying gas flow with variable physical properties *Int. J. Heat Mass Transfer* **28**(1) 59–68 (1985)